

grated circuits can be usefully transferred to chemical and biochemical analysis and processing in microfluidic devices.

The two devices presented here illustrate that complex fluidic circuits with nearly arbitrary complexity can be fabricated using microfluidic LSI. The rapid, simple fabrication procedure combined with the powerful valve multiplexing can be used to design chips for many applications, ranging from high-throughput screening applications to the design of new liquid display technology. The scalability of the process makes it possible to design robust microfluidic devices with even higher densities of functional valve elements, so that the ultimate complexity and application are limited only by one's imagination.

References and Notes

1. T. R. Reid, *The Chip: How Two Americans Invented the Microchip and Launched a Revolution* (Simon & Schuster, New York, 1984).
2. A. G. Hadd, S. C. Jacobson, J. M. Ramsey, *Anal. Chem.* **71**, 5206 (1999).
3. D. J. Harrison *et al.*, *Science* **261**, 895 (1993).
4. P. C. H. Li, D. J. Harrison, *Anal. Chem.* **69**, 1564 (1997).
5. A. G. Hadd, D. E. Raymond, J. W. Haliwell, S. C. Jacobson, S. C. Ramsey, *Anal. Chem.* **69**, 3407 (1997).
6. E. T. Lagally, I. Medintz, R. A. Mathies, *Anal. Chem.* **73**, 565 (2001).
7. J. Khandurina *et al.*, *Anal. Chem.* **72**, 2995 (2000).
8. E. Eteshola, D. Leckband, *Sens. Actua. B* **72**, 129 (2001).
9. J. Wang, A. Ibanez, M. P. Chatrathi, A. Escarpa, *Anal. Chem.* **73**, 5323 (2001).
10. M. A. Unger, H.-P. Chou, T. Thorsen, A. Scherer, S. R. Quake, *Science* **288**, 113 (2000).
11. Master molds for the microfluidic channels are made by spin-coating positive photoresist (Shipley SJR 5740) on silicon (9 μm high) and patterning them with high-resolution (3386 dpi) transparency masks. The channels on the photoresist molds are rounded at 120°C for 20 min to create a geometry that allows full valve closure. The devices were fabricated by bonding together two layers of two-part cure silicone (Dow Corning Sylgard 184) cast from the photoresist molds. The bottom layer of the device, containing the flow channels, is spin-coated with 20:1 part A:B Sylgard at 2500 rpm for 1 min. The resulting silicone layer is $\sim 30 \mu\text{m}$ thick. The top layer of the device, containing the control channels, is cast as a thick layer ($\sim 0.5 \text{ cm}$ thick) with 5:1 part A:B Sylgard using a separate mold. The two layers are initially cured for 30 min at 80°C. Control channel interconnect holes are then punched through the thick layer (released from the mold), after which it is sealed, channel side down, on the thin layer, aligning the respective channel networks. Bonding between the assembled layers is accomplished by curing the devices for an additional 45 to 60 min at 80°C. The resulting multilayer devices are cut to size and mounted on RCA cleaned No. 1, 25 mm square glass coverslips, or onto coverslips spin-coated with 5:1 part A:B Sylgard at 5000 rpm, and cured at 80°C for 30 min, followed by incubation at 80°C overnight.
12. L. Buchailot, E. Farnault, M. Hoummady, H. Fujita, *Jpn. J. Appl. Phys.* **2** **36**, L794 (1997).
13. The control channels are dead end-filled with water before actuation with pneumatic pressure; the compressed air at the ends of the channels is forced into the bulk porous silicone. This procedure eliminates gas transfer into the flow layer upon valve actuation, as well as evaporation of the liquid contained in the flow layer.
14. H. P. Chou, C. S. Spence, A. Scherer, S. R. Quake, *Proc. Natl. Acad. Sci. U.S.A.* **96**, 11 (1999).
15. V. Linder, E. Verpoorte, W. Thormann, N. F. de Rooij, H. Sigrist, *Anal. Chem.* **73**, 4181 (2001).
16. T. Yang, S. Jung, H. Mao, P. S. Cremer, *Anal. Chem.* **73**, 165 (2001).
17. D. C. Duffy, J. C. MacDonald, O. J. A. Schueller, G. M. Whitesides, *Anal. Chem.* **70**, 4974 (1998).
18. B. A. Grzybowski, R. Haag, N. Bowden, G. M. Whitesides, *Anal. Chem.* **70**, 4645 (1998).
19. We thank M. Enzelberger, C. Hansen, M. Adams, and M. Unger for helpful discussions. Supported in part by Army Research Office grant DAAD19-00-1-0392 and by the DARPA Bioflips program.

M. Unger for helpful discussions. Supported in part by Army Research Office grant DAAD19-00-1-0392 and by the DARPA Bioflips program.

5 August 2002; accepted 17 September 2002

Published online 26 September 2002;

10.1126/science.1076996

Include this information when citing this paper.

Self-Assembly of Highly Phosphorylated Silaffins and Their Function in Biosilica Morphogenesis

Nils Kröger,¹ Sonja Lorenz,² Eike Brunner,² Manfred Sumper^{1*}

Silaffins are uniquely modified peptides that have been implicated in the biogenesis of diatom biosilica. A method that avoids the harsh anhydrous hydrogen fluoride treatment commonly used to dissolve biosilica allows the extraction of silaffins in their native state. The native silaffins carry further posttranslational modifications in addition to their polyamine moieties. Each serine residue was phosphorylated, and this high level of phosphorylation is essential for biological activity. The zwitterionic structure of native silaffins enables the formation of supramolecular assemblies. Time-resolved analysis of silica morphogenesis *in vitro* detected a plastic silaffin-silica phase, which may represent a building material for diatom biosilica.

Diatoms are unicellular, eukaryotic algae that produce a wide variety of nanopatterned silica structures in a genetically controlled manner (1). Biosilica morphogenesis is an extremely rapid process that is accomplished under mild physiological conditions, thus exceeding the capabilities of present-day materials engineering. Elucidating the molecular mechanisms of biosilica formation is therefore expected to help researchers devise new synthetic routes to nanostructured silica materials (2, 3).

Recently, silaffins and long-chain polyamines have been identified as constituents of biosilica and shown to accelerate silica formation from a monosilicic acid solution *in vitro* (4, 5). On the basis of the physicochemical properties of polyamines, a phase separation model has been proposed that is able to explain the nanopatterning of biosilica (6). Silaffins are peptides that carry numerous posttranslational modifications. The silaffins from *Cylindrotheca fusiformis* contain lysine residues that are linked by their ϵ -amino groups to long-chain polyamines (7). It is due to this modification that silaffin peptides can precipitate silica nanospheres at mildly acidic pH conditions (4), which likely represent the physiologically relevant pH range (8).

Previously, the extraction and purification of silaffins has been achieved by the treatment of diatom shells with anhydrous hydrogen fluoride

(HF), a treatment known to cleave O-glycosidic and phosphate ester bonds (9). However, silaffins contain a high percentage of hydroxyamino acids, candidates for posttranslational modifications. Therefore, the silaffins extracted to date may have lost functional modifications of hydroxyamino acids. To address this concern and to be able to study silica precipitation activities of native silaffins, we developed a gentler method for silaffin extraction. We found that native silaffins carry additional modifications that proved to be essential for biosilica formation.

It has previously been shown that an acidic aqueous solution of ammonium fluoride is capable of dissolving diatom biosilica (10) by converting silica into soluble ammonium hexafluorosilicate. When *C. fusiformis* cell walls are treated with an aqueous solution of ammonium fluoride at pH = 5, the complete set of silaffins and long-chain polyamines is solubilized. The apparent molecular masses of all silaffin species present in the aqueous ammonium fluoride extract are shifted toward higher molecular masses, indicating the existence of HF-labile modifications (11). An abundant peptide (apparent molecular mass of 6.5 kD) was purified from the ammonium fluoride extract (Fig. 1, lane 1) (12). After an additional treatment with anhydrous HF, this peptide exhibited a much higher electrophoretic mobility and comigrated in SDS-polyacrylamide gel electrophoresis (SDS-PAGE) with silaffin-1A (Fig. 1, lanes 2, 3), which has previously been characterized from HF-extracted cell walls (4). NH₂-terminal amino acid sequencing of this material resulted in the sequence SXXSGSYSGS (G, Gly; S, Ser; Y, Tyr; X, modified lysine residue)

¹Lehrstuhl Biochemie I, ²Institut für Biophysik und Physikalische Biochemie, Universität Regensburg, 93053 Regensburg, Germany.

*To whom correspondence should be addressed. E-mail: manfred.sumper@vkl.uni-regensburg.de

REPORTS

that is diagnostic of silaffin-1A. Because treatment with an aqueous ammonium fluoride solution is highly unlikely to remove any covalent amino acid modification, the 6.5-kD peptide is expected to represent the native form of silaffin-1A and is thus termed natSil-1A.

To elucidate the chemical nature of the HF-sensitive modifications in natSil-1A, we subjected the purified peptide to elemental analysis by energy dispersive X-ray analysis (EDXA) in a field emission scanning electron microscope (FESEM) (12). This analysis revealed a substantial amount of phosphorus in natSil-1A that is absent in silaffin-1A, suggesting phosphorylation of the numerous hydroxyamino acids of the peptide backbone. After ashing (13) natSil-1A, about 8 mol of phosphate per mol of natSil-1A were found. With the use of mass spectroscopy, natSil-1A isoforms (variations in polyamine chain length) exhibited a mass increase of 640 D as compared to the corresponding silaffin-1A₁ peptides (7, 12). This difference perfectly matches the molecular mass of eight phosphate groups attached to silaffin-1A₁ peptides.

The attachment sites of the phosphate groups within natSil-1A₁ were analysed by ³¹P nuclear magnetic resonance (NMR) spectroscopy. The NMR spectrum (Fig. 1B) revealed the presence of four intense signals at 1.8 to 2.2 ppm, which can be assigned to phosphorylated serine residues (12), and a further intense signal at 0.82 ppm. As is evident from comparison of the ¹H-decoupled and the nondecoupled spectra (Fig.

1B), the signal at 0.82 ppm is consistent with the structure of phosphorylated trimethyl-hydroxylysine (12). This lysine derivative has previously been identified as a common organic constituent in cell walls from many diatom species, including *C. fusiformis* (14). The signal ratio of the phosphorylated serine and trimethyl-hydroxylysine residues is 7 to 1, indicating that all seven serine residues in natSil-1A₁ are phosphorylated.

Taken together, these data define the structure of natSil-1A₁ (Fig. 1C). Eleven of the 15 amino acid residues are modified by ionized groups, introducing an extreme accumulation of both positive and negative charges. On the basis of earlier work (7), natSil-1A should also contain minor amounts of material derived from the related peptide silaffin-1A₂. A more detailed analysis of natSil-1A by reversed-phase high-performance liquid chromatography (RP-HPLC) and electrospray ionization mass spectroscopy (ESI-MS) revealed the presence of minor amounts (about 20%) of phosphorylated derivatives of silaffin-1A₂ (11).

Previously, silica precipitation experiments were performed in vitro with a phosphate-containing buffer (4, 5, 7). To determine any effect of phosphate anions on silaffin-induced silica formation, we replaced the phosphate buffer with a sodium acetate buffer (12). NatSil-1A retained its activity to precipitate silica from a monosilicic acid solution. Within 10 min, an average of 86.5 (± 6) nmol silica was formed per nmol of added peptide (Fig. 2, black line). The precipitate consisted of nanospheres with diameters between 400 and 700 nm that ap-

peared to be independent from each other and were rarely interconnected (Fig. 2, inset). Under the same conditions, silaffin-1A was incapable of precipitating silica (Fig. 2, green line), indicating that phosphate is required. Silica precipitation activity of silaffin-1A was restored by adding phosphate to the solution. In the presence of 30 mM phosphate, silaffin-1A precipitated the same amount of silica as natSil-1A under phosphate-free conditions (Fig. 2, red line). However, at low phosphate concentrations (3 mM), silaffin-1A precipitated significantly less silica than natSil-1A, and the amount of precipitated silica reached a plateau value with increasing silaffin-1A concentrations (Fig. 2, blue

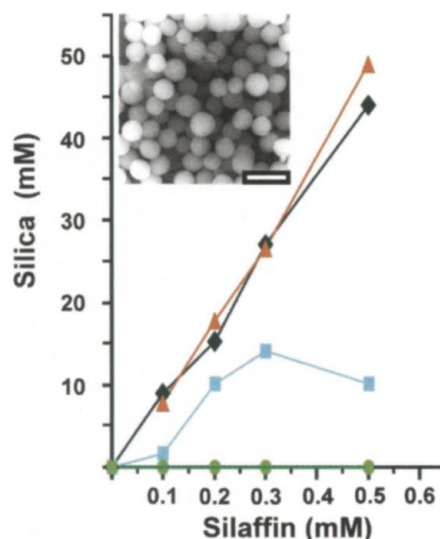


Fig. 2. Silaffin-induced silica precipitation. The diagram exhibits the correlation between the amount of silaffin added to a buffered monosilicic acid solution (50 mM sodium acetate, pH = 5.5) and the amount of precipitated silica. Lines indicate silica precipitation using natSil-1A (black), silaffin-1A (green), silaffin-1A in the presence of 30 mM phosphate (red), and silaffin-1A in the presence of 3 mM phosphate (blue). (Inset) SEM micrograph of the precipitate formed by 0.3 mM natSil-1A (scale bar, 1 μm).

Fig. 1. Structural analysis of natSil-1A. (A) Tricine-SDS-PAGE analysis (22) of silaffins from *C. fusiformis*. Lane 1, 6.5-kD component isolated from cell walls after ammonium fluoride extraction (12); lane 2, purified 6.5-kD component after treatment with anhydrous HF; lane 3, silaffins extracted from cell walls with anhydrous HF (bands from top to bottom: silaffin-2, silaffin-1B, silaffin-1A, long-chain polyamines). (B) ³¹P NMR spectra of 0.2 mM natSil-1A dissolved in 200 mM sodium citrate, pH = 5.0 (202.4 MHz resonance frequency, 20 s repetition time). Spectra were measured without (top, 7168 scans) and with (bottom, 4096 scans) ¹H-decoupling at room temperature, using 85% H₃PO₄ as an external reference. Linewidth of the signal at 0.82 ppm in the ¹H-decoupled spectrum is 8.4 Hz. (C) Schematic chemical structure of natSil-1A₁. The annotation of charges within the molecule is tentative for a solution around pH = 5. Most likely, not all amino groups are protonated, because the basicity of amino groups is reduced due to mutual repulsion of the positive charges within the polyamine chains (23).

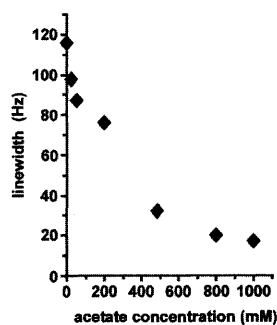
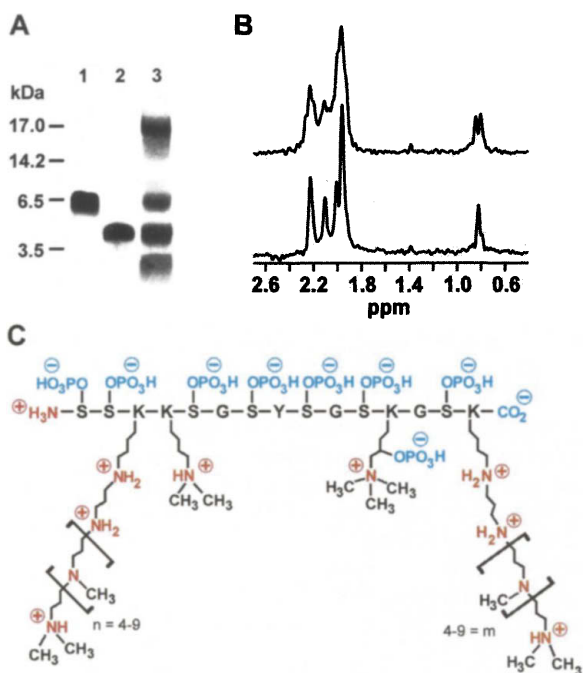


Fig. 3. Dependence of ³¹P NMR linewidth of natSil-1A on the salt concentration. The linewidth (full width at half maximum) of the trimethyl-hydroxylysine phosphate signal in ¹H-decoupled ³¹P NMR spectra is plotted against the buffer concentration (sodium acetate, pH = 5.5) present in the natSil-1A solution.

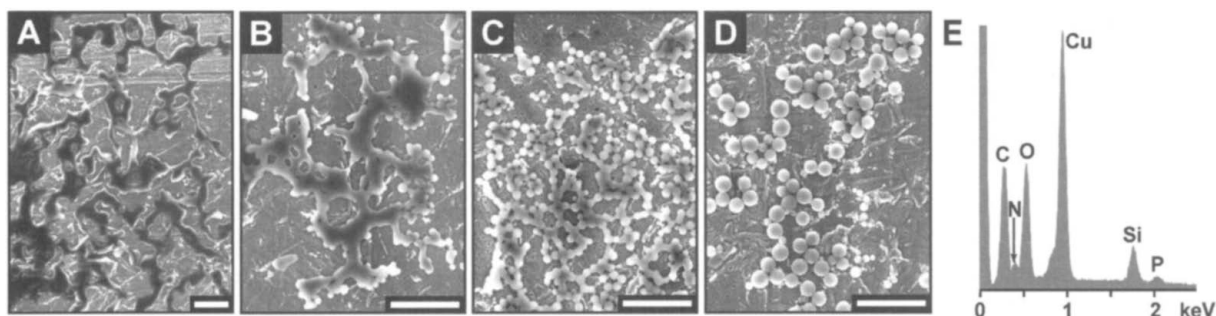


Fig. 4. Time-resolved analysis of silica morphogenesis in vitro. SEM images of silica structures formed (A) 3.5 min, (B) 4.5 min, (C) 5 min, and (D) 8 min after the addition of natSil-1A to a buffered monosilicic acid solution (50 mM sodium

acetate, pH = 5.5). Scale bars, 2 μ m. (E) Elemental composition of silica structures in (A) as determined by EDXA. C, N, and P signals are diagnostic for natSil-1A. The strong Cu signal is caused by the sample holder (copper grid).

line). This demonstrates that phosphate becomes the limiting factor. Therefore, we conclude that the numerous phosphate groups in natSil-1A serve as an intrinsic source of anions required for silica formation by diatoms.

The zwitterionic structure of natSil-1A (polyamine moieties and phosphate groups) is likely to cause a self-assembly process via electrostatic interactions. To investigate this possibility, we analyzed by ^{31}P NMR spectroscopy the aggregation behavior of natSil-1A at pH = 5.5. If natSil-1A molecules self-assemble, a broadening of ^{31}P NMR linewidths is expected that depends on aggregate size (15). As exemplified for the signal of phosphorylated trimethyl-hydroxylysine, the linewidth of this signal is strongly dependent on the ionic strength (Fig. 3). The linewidth strongly decreases with increasing salt concentrations. This effect demonstrates that natSil-1A molecules do indeed form large aggregates via electrostatic interactions. At low ionic strength, an aggregate size of at least 700 molecules can be estimated from the broadening of ^{31}P NMR linewidths (12, 16). We hypothesize that silaffin self-assembly is a prerequisite for biosilica formation, because such assemblies might provide the template for silicic acid polycondensation. This would explain the inability of silaffin-1A to promote silica precipitation in the absence of phosphate. In contrast to natSil-1A, silaffin-1A molecules do not have the zwitterionic structure and therefore are unlikely to form aggregates. The addition of phosphate anions restores the silica precipitation activity of silaffin-1A, presumably because phosphate anions serve as ionic cross-linkers promoting the aggregation of polycationic silaffin-1A molecules.

The large silica nanospheres (400 to 700 nm in diameter) formed by natSil-1A in vitro (Fig. 2, inset) do not represent biologically relevant structures. Diatom biosilica is composed of particles that are only 10 to 100 nm in diameter (17–20). However, the large spheres may only represent the artificial end product (due to in vitro conditions) of a morphogenetic process that starts out from biologically relevant silica structures. To investigate this possibility, we followed by scanning electron microscopy (SEM) the time dependence of natSil-1A-in-

duced silica formation in vitro. Silica formation was initiated in a test tube by adding monosilicic acid to a buffered, phosphate-free solution of natSil-1A (time $t = 0$ min). At regular time intervals, aliquots were withdrawn from the test tube and investigated for silica-containing structures by FESEM and EDXA (11). The first structures to be observed ($t = 3$ to 4 min) were extended flat networks of a branched, irregularly shaped phase (Fig. 4A). EDXA confirmed that these networks contained both silica and natSil-1A (Fig. 4E). Within only 2 min, spherical particles bud from the edges of this composite ($t = 4.5$ min, Fig. 4B). Simultaneously, bands with almost equidistant pinches (spacing ~ 300 nm) develop, giving the appearance of strands of intimately connected spheres ($t = 5$ min, Fig. 4C). As pinching progresses, size differences between neighboring spheres become more pronounced, suggesting that some spheres grow by the consumption of others. At later stages ($t = 8$ min, Fig. 4D), neighboring spheres are attached only by small necks and large differences in sphere sizes are observed, ranging from 100 nm up to 600 nm. Eventually ($t \geq 10$ min) the budding process is complete, and large, independent silica spheres predominate (diameters 400 to 700 nm).

These observations show that the large silica nanospheres are produced from an irregularly shaped network of an apparently plastic silicanatSil-1A phase. It seems likely that the formation of the silica-natSil-1A phase (Fig. 4A), rather than its conversion to large spheres, is an important step of in vivo biosilica morphogenesis in *C. fusiformis*. The formation of biosilica in diatoms takes place within a membrane-bound compartment (silica deposition vesicle) that acts as a casting mold (21). The plastic natSil-1A-silica phase observed in vitro may represent the moldable biosilica material used to form the solid silica elements (girdle bands, central nodule, and fibulae) of *C. fusiformis* that do not exhibit any patterning by nanosized pores.

The structures of in vitro silica precipitates were previously shown to be strongly influenced by combining different silaffins (4). Accordingly, when additional native silaffins be-

come available, combinations of these proteins may achieve an even more controlled process of silica formation.

References and Notes

1. F. Round, R. Crawford, D. Mann, *The Diatoms* (Cambridge Univ. Press, Cambridge, UK, 1990).
2. S. Mann, G. Ozin, *Nature* **382**, 313 (1996).
3. J. Parkinson, R. Gordon, *Trends Biotechnol.* **17**, 190 (1999).
4. N. Kröger, R. Deutzmann, M. Sumper, *Science* **286**, 1129 (1999).
5. N. Kröger, R. Deutzmann, C. Bergsdorf, M. Sumper, *Proc. Natl. Acad. Sci. U.S.A.* **97**, 14133 (2000).
6. M. Sumper, *Science* **295**, 2430 (2002).
7. N. Kröger, R. Deutzmann, M. Sumper, *J. Biol. Chem.* **276**, 26066 (2001).
8. E. G. Vrieling, W. W. C. Gieskes, T. P. M. Beelen, *J. Phycol.* **35**, 548 (1999).
9. A. J. Mort, D. T. A. Lamport, *Anal. Biochem.* **82**, 289 (1977).
10. D.M. Swift, A. P. Wheeler, *J. Phycol.* **28**, 202 (1992).
11. N. Kröger, M. Sumper, data not shown.
12. Materials and methods are available as supporting material on Science Online.
13. J. E. Buss, J. T. Stull, *Meth. Enzymol.* **99**, 7 (1983).
14. T. Nakajima, B. E. Volcani, *Biochem. Biophys. Res. Comm.* **39**, 28 (1970).
15. J. Cavanagh, W. J. Fairbrother, A. G. Palmer III, N. J. Skelton, *Protein NMR Spectroscopy* (Academic Press, San Diego, CA, 1996).
16. The ^{31}P NMR linewidth (full width at half maximum) served to estimate the correlation time for cluster reorientation from which the hydrodynamic radius of a natSil-1A cluster was calculated. The specific volume of a natSil-1A molecule was estimated by molecular modeling.
17. M. L. Chiappino, B. E. Volcani, *Protoplasma* **93**, 205 (1977).
18. A. M. M. Schmid, D. Schulz, *Protoplasma* **100**, 267 (1979).
19. S. A. Crawford, M. J. Higgins, P. Mulvaney, R. Wetherbee, *J. Phycol.* **37**, 1 (2001).
20. F. Noll, M. Sumper, N. Hampp, *Nano. Lett.* **2**, 91 (2002).
21. J. Pickett-Heaps, A. M. M. Schmid, L. A. Edgar, in *Progress in Phycolological Research*, F. E. Round, D. J. Chapman, Eds. (Biopress, Bristol, UK, 1990), vol. 7, pp. 1–169.
22. H. Schägger, G. von Jagow, *Anal. Biochem.* **166**, 368 (1987).
23. A. Bencini, A. Bianchi, E. Garcia-Espana, M. Micheloni, J. A. Ramirez, *Coord. Chem. Rev.* **188**, 97 (1999).
24. We thank R. Deutzmann and E. Hochmuth for MS analysis and G. Lehmann for technical assistance. Supported by the Deutsche Forschungsgemeinschaft (grants SFB 521-A2 and -A6) and the Fonds der Chemischen Industrie.

Supporting Online Material

www.sciencemag.org/cgi/content/full/298/5593/584/DC1

Materials and Methods

16 July 2002; accepted 5 September 2002